Spectrum Analysis with Adaptive Precision for Space Vector Pulse Width Modulation

Guoqiang Chen and Jianli Kang

*School of Mechanical and Power Engineering, Henan Polytechnic University,
Jiaozuo, 454000, China
jz97cgq@sina.com*

Abstract

Aiming at the problem that the theoretical spectrum expression of the output voltage waveform in the space vector pulse width modulation strategy is often extremely complicated, most tedious and quite error-prone, the study develops a universal procedure and algorithm with adaptive precision to analyze the harmonic spectrum. The key steps and technique of the procedure and algorithm are given firstly. The algorithm steps include storing the switching states and the vector sequences, computing the basic space vector duration time, storing the duration time, sampling output voltage values and computing the spectrum using the fast Fourier transform algorithm. The sampling number doubles in each iteration for the next iteration. The adaptive precision is realized through controlling the amplitude or magnitude error between the current result and the previous result. The realization method and the key codes are presented secondly. Finally, three numerical experiments are presented to verify the developed algorithm, and the results verify its correctness, reliability and convenience.

Keywords: space vector pulse width modulation, spectrum analysis, fast Fourier transformation, adaptive precision

1. Introduction

The space vector pulse width modulation (SVPWM) strategy is an important subclass in the family of pulse width modulation (PWM) technology, and has been widely used in all kinds of fields that require the power source conversion from the direct current(DC) source to the alternating current(AC) one [1-2]. Because of the simple structure and load characteristic, the voltage source inverter has gained wide application. From the aspect of output voltage, the output of the inverter is voltage pulse series. Because the fundamental of SVPWM technology is the volt-second balance principle, the undesirable harmonic is inevitable besides the required fundamental one [2-4]. The harmonic has heavy effects on the application, such as loss, dynamic characteristic of the motor system, electromagnetic compatibility and audible noise [5-14]. Therefore, spectrum analysis for the harmonic is a necessary task in assessing and improving a new SVPWM strategy. The theoretical spectrum expression of the inverter output voltage and current is often extremely complicated, and the magnitudes of the harmonics always include the summation of the infinite series [2-15]. Huge differences in the spectrum expression exist in different SVPWM strategies. To a new strategy, the deducing process is very difficult, most tedious and quite error-prone, and the explicit expression cannot be usually gotten. An analysis method is therefore needed of which the harmonic spectrum can be computed using a universal procedure and algorithm with required precision [16]. In this paper, a new spectrum analysis algorithm with adaptive precision is proposed; the key steps and analysis procedure are presented, and several SVPWM strategies are analyzed using the proposed algorithm to verify its correctness, reliability and convenience.

2. SVPWM Technology

The principle of the multi-level three-phase inverter is shown in Figure 1 [4, 17-19]. The DC bus voltage is U_{DC}. A K -level inverter gives K voltage levels with respect to the negative rail N.
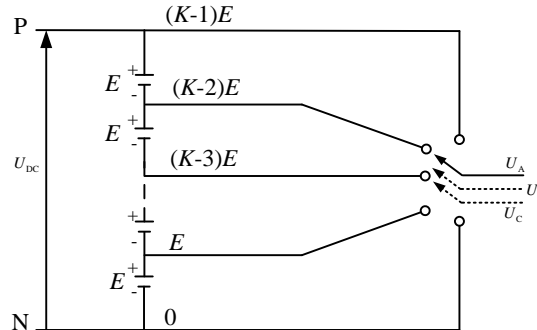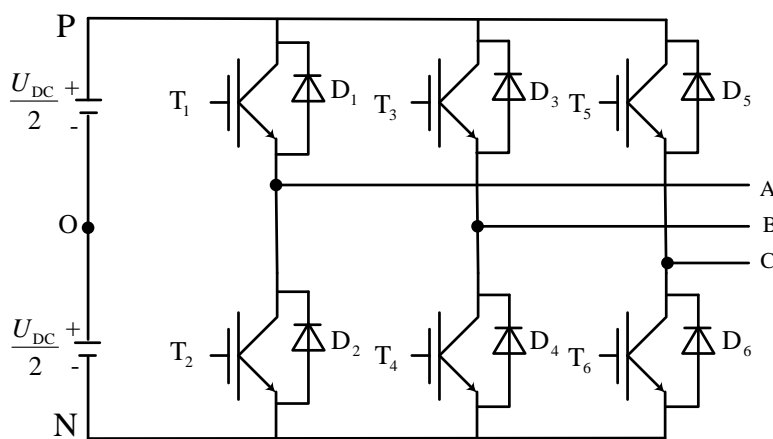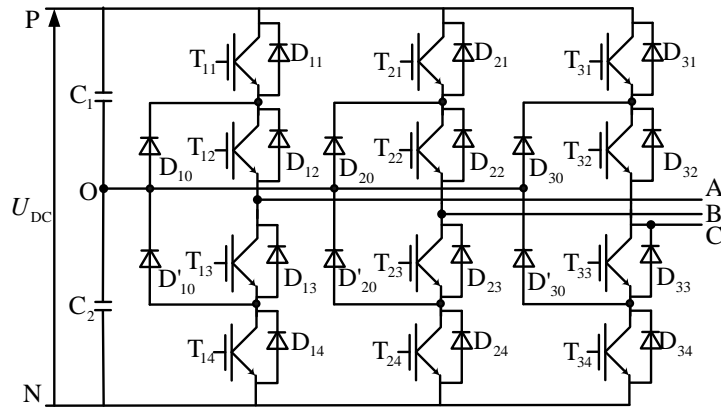

Figure 1. Multi-Level Three-Phase Inverter Principle

The topologies of the classic two-level inverter and the three-level inverter are shown in Figure 2. For example, a two-level inverter, as shown in Figure 2(a), gives two voltage levels (0 and U_{DC}) with respect to the negative rail N or ($-U_{DC}/2$ and $U_{DC}/2$) with respect to the neutral point O. The inverter has 8 permissible states that are corresponding to the 8 basic space vectors as shown in Figure 3(a). An arbitrary command/reference voltage vector $\vec{U}_s$ with the vector amplitude $U_\circ$ and the phase angle θ inside the hexagon region shown in Figure 3(a) can be generated by two adjacent active vectors ($\vec{U}_1$ and $\vec{U}_2$ in the first sextant) and the zero vectors. The on-state duration times T_1 , T_2 and T_0 of the three vectors are determined by the identical voltseconds balance at the periodical time interval T_s using Equation (1). There are large numbers of vector operation modes that satisfy this equation.

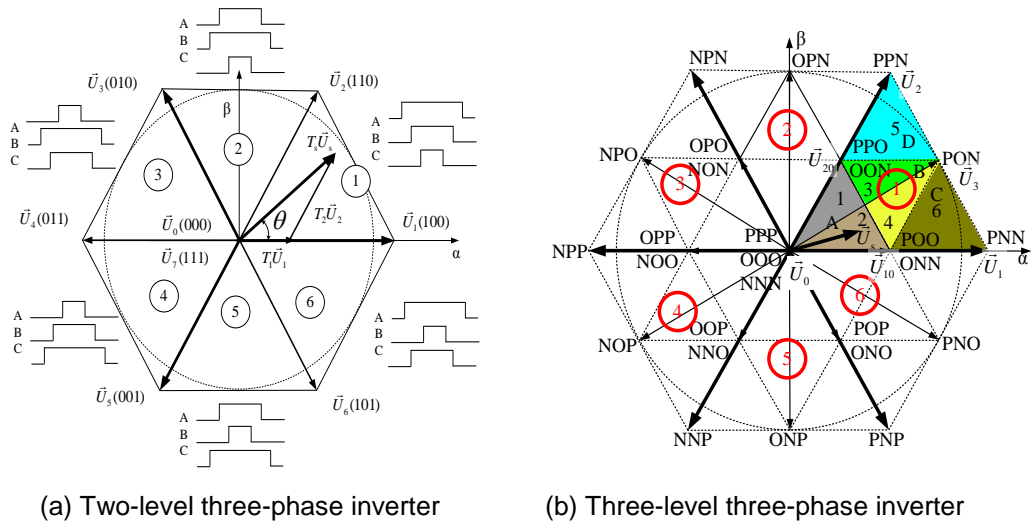$$T_s\vec{U}_s = T_1\vec{U}_1 + T_2\vec{U}_2 \tag{1}$$

(a) Two-level three-phase inverter

(b) Three-level three-phase inverter

Figure 2. The Topologies of the Two-Level Inverter and the Three-Level Inverter

The three-level neutral-point clamped(NPC) inverter, as shown in Figure 3(b), gives three voltage levels (0, $U_{DC}/2$ and U_{DC}) with respect to the negative rail N or ($-U_{DC}/2$, 0 and $U_{DC}/2$) with respect to the neutral point O created by two identical DC link capacitors C_1 and C_2. The corresponding space vectors for the 27 states are shown in Figure 3(b). An arbitrary command/reference voltage vector $\vec{u}_s$ can be generated by three vectors corresponding to the apexes of the triangle that includes $\vec{u}_s$. For example, the three vectors are PPP/OOO/NNN, POO/ONN and POO/ONN, as shown in Figure 3(b).

(a) Two-level three-phase inverter   (b) Three-level three-phase inverter

Figure 3. The Vector Diagram of the Three-Phase Inverter. The Notations P, O and N Refer to That the Three Phase Output Terminals Are Positive, Zero and Negative, Respectively

3. Spectrum Analysis Algorithm with Adaptive Precision

3.1. Key Steps in the Algorithm

The algorithm for the spectrum analysis with adaptive precision is as follows.
Step 1: Store the switching states and vector sequences in a vector sequence matrix S.

Step 2: Compute the duration times of the basic space vectors that are used to generate the command/reference voltage vector.

Step 3: Store the duration times of the basic space vectors in Step 2 in a time matrix ST.

Step 4: Sample the output waveform of the inverter and compute the spectrum using the Fast Fourier Transform (FFT) algorithm.

3.2. The Vector Sequence Matrix S and the Time Matrix ST

In step 1, the vector sequence matrix S including 3 rows that stores the voltage level coefficients of the corresponding basic space vectors. The first row is used for phase-A, the second row is used for phase-B, and the third row is used for phase-C. The integer N is odd and is not less than 3. All the values of the possible voltage level coefficients are $(N-1)/2$, $(N-1)/2-1$, $(N-1)/2-2$, $\cdots$, 2, 1, 0, -1, -2, $\cdots$, $-[(N-1)/2-2]$, $-[(N-1)/2-1]$, $-(N-1)/2$ for an N-level inverter, while $(N-1)/2$, $(N-1)/2-1$, $(N-1)/2-2$, $\cdots$, 2, 1, -1, -2, $\cdots$, $-[(N-1)/2-2]$, $-[(N-1)/2-1]$, $-(N-1)/2$ for an N-1-level inverter. The benchmark of the voltage level is $U_{DC}/(N-1)$. That is to say, $U_{DC}/2$ is for both the two-level inverter and the three-level inverter.

For example, for the commonly used symmetrical 7-segment pulse pattern of the two-level inverter, the corresponding matrix SD that should be concatenated to the vector sequence matrix S. In the first sextant the matrix SD is

$$SD = \begin{bmatrix} -1 & 1 & 1 & 1 & 1 & 1 & -1 \\ -1 & -1 & 1 & 1 & 1 & -1 & -1 \\ -1 & -1 & -1 & 1 & -1 & -1 & -1 \end{bmatrix} \tag{2}$$

The duration times for the two basic active space vector in the first sextant are

$$\begin{cases} T_1 = \dfrac{\sqrt{3}}{2} M T_s \sin\left(\pi/3 - \theta\right) \\ T_2 = \dfrac{\sqrt{3}}{2} M T_s \sin\theta \end{cases} \tag{3}$$

where M is the modulation index corresponding to the command/reference voltage vector, θ is the phase angle of the command/reference voltage vector, and T_s is the switching period.

The total duration time of the two zero vectors (T_{00} for $\vec{U}_0$ and T_{07} for $\vec{U}_7$) is

$$T_0 = T_s - T_1 - T_2 = T_{00} + T_{07} \tag{4}$$

The corresponding matrix STD that should be concatenated to the time matrix ST is

$$STD = [T_0/4 \quad T_1/2 \quad T_2/2 \quad T_0/2 \quad T_2/2 \quad T_1/2 \quad T_0/4] \tag{5}$$

The on-state duration times of the basic vectors for the three-level inverter in the first sextant are

$$\begin{cases} T_0 = \left[1 - \sqrt{3}M \sin\left(\pi/3 + \theta\right)\right] T_s \\ T_{10} = \sqrt{3}M T_s \sin\left(\pi/3 - \theta\right) \qquad \text{(Triangle A)} \\ T_{20} = \sqrt{3}M T_s \sin\theta \end{cases} \tag{6}$$

$$\begin{cases} T_{10} = \left(1 - \sqrt{3}M \, \sin\theta\right)T_s \\ T_{20} = \left[1 - \sqrt{3}M \, \sin\left(\pi/3 - \theta\right)\right]T_s \qquad \text{(Triangle B)} \\ T_3 = \left[\sqrt{3}M \, \sin\left(\pi/3 + \theta\right) - 1\right]T_s \end{cases} \qquad (7)$$

$$\begin{cases} T_{10} = \left[2 - \sqrt{3}M \, \sin\left(\pi/3 + \theta\right)\right]T_s \\ T_3 = \sqrt{3}M T_s \sin\theta \qquad \text{(Triangle C)} \\ T_1 = \left[\sqrt{3}M \, \sin\left(\pi/3 - \theta\right) - 1\right]T_s \end{cases} \qquad (8)$$

$$\begin{cases} T_3 = \sqrt{3}M T_s \sin\left(\pi/3 - \theta\right) \\ T_2 = \left(\sqrt{3}M \, \sin\theta - 1\right)T_s \qquad \text{(Triangle D)} \\ T_{20} = \left[2 - \sqrt{3}M \, \sin\left(\pi/3 + \theta\right)\right]T_s \end{cases} \qquad (9)$$

In the triangle A(1) the corresponding matrix SD is

$$SD = \begin{bmatrix} 1 & 1 & 0 & 0 & 0 & 1 & 1 \\ 1 & 0 & 0 & 0 & 0 & 0 & 1 \\ 0 & 0 & 0 & -1 & 0 & 0 & 0 \end{bmatrix} \qquad (10)$$

In the triangle A(2) the corresponding matrix SD is

$$SD = \begin{bmatrix} 1 & 0 & 0 & 0 & 0 & 0 & 1 \\ 0 & 0 & 0 & -1 & 0 & 0 & 0 \\ 0 & 0 & -1 & -1 & -1 & 0 & 0 \end{bmatrix} \qquad (11)$$

For the control factor k_c the corresponding matrix STD is

$$STD = \begin{bmatrix} k_c T_{20}/2 & T_{10}/2 & T_0/2 & (1 - k_c)T_{20} & T_0/2 & T_{10}/2 & k_c T_{20}/2 \end{bmatrix} \qquad (12)$$

3.3. The Detailed Procedure of Step 4

The Step 4 can be divided into several sub-steps as follows.

Step 41: The output voltage pulse series is sampled according to the vector sequence matrix S in Step 1 and the time matrix ST in Step 3, and then a discrete time sequence DS can be got.

Step 411: Compute the cumulative sum of the elements of the time matrix ST and store the cumulative sum in a cumulative time matrix STC. The q-th element of the cumulative time matrix STC is got through Equation (13).

$$STC[q] = \sum_{i=1}^{q} STC[i] \qquad (13)$$

Step 412: The sampling time of the r-th element of the discrete time sequence DS is corresponding to the k-th element of the cumulative time matrix STC. The index k is determined using Equation (14) with the time sampling interval Δ_t.

$$\left| \frac{STC[k] - ST[k]}{\Delta_t} \right| < r \le \left| \frac{STC[k]}{\Delta_t} \right| \tag{14}$$

Step 413: Sample the voltage value according the k-th element of the vector sequence matrix S.

Step 42: The representation in the frequency domain of DS is got using FFT algorithm. Let the Q discrete amplitude values are $A_1, A_2, A_3, \cdots, A_Q$ and the Q discrete phase values are $\varphi_1, \varphi_2, \varphi_3, \cdots, \varphi_Q$.

Step 43: Precision control and processing.

Step 431: If it is the first time for sampling and computing the frequency spectrum, go to Step 435.

Step 432: If this is not the first time for sampling and computing the frequency spectrum, the difference values between the current spectrum $A_1, A_2, A_3, \cdots, A_Q$, $\varphi_1, \varphi_2, \varphi_3, \cdots, \varphi_Q$ and the last spectrum $A_{01}, A_{02}, A_{03}, \cdots, A_{0Q}$, $\varphi_{01}, \varphi_{02}, \varphi_{03}, \cdots, \varphi_{0Q}$. Go to Step 433.

$$\begin{cases} \Delta A_i = A_i - A_{0i} \\ \Delta \varphi_i = \varphi_i - \varphi_{0i} \end{cases} \qquad (i = 1, 2, 3 \cdots, Q) \tag{15}$$

Step 433: If $\max(|\Delta A_i|)$ is more than the set amplitude error limit or $\max(|\Delta \varphi_i|)$ is more than the set phase error limit, go to Step 435.

Step 434: If $\max(|\Delta A_i|)$ is not more than the set amplitude error and $\max(|\Delta \varphi_i|)$ is not more than the set phase error, go to Step 436.

Step 435: Double the sampling number. Go to Step 41.

Step 436: Go to 44.

Step 44: Store the last discrete amplitude values and phase values.

Another feasible criterion can also be utilized in Step 432. A relative magnitude error of the harmonic should be defined as

$$\Delta A_{ri} = \frac{A_i}{A_1} - \frac{A_{0i}}{A_{01}} \qquad (i = 1, 2, 3 \cdots, Q) \tag{16}$$

In this criterion the ΔA_i and $\Delta \varphi_i$ are replaced by ΔA_{ri}.

4. Realization in MATLAB

MATLAB is a powerful tool for the numerical computation and result presentation. Many powerful functions in MATLAB can be utilized directly to make the proposed algorithm highly efficient, simple and convenient. The key codes and technique on realization in MATLAB are presented as follows based on the two-level inverter.

4.1. Basic Space Vectors Storage

The values of the possible voltage level coefficients of the 8 basic space vectors are stored in a 3-by-8 matrix using the code as follows. The 8 rows are corresponding to the 8 active space vectors ($\vec{U}_1(100), \vec{U}_2(110), \vec{U}_3(010), \vec{U}_4(011), \vec{U}_5(001)$ and $\vec{U}_6(101)$) and the two zero vectors ($\vec{U}_0(000)$ and $\vec{U}_7(111)$).

```
myV=[ 1  -1  -1;  1   1  -1;   -1   1  -1;  -1   1   1; -1  -1   1 ;1 -1   1;  -1  -1  -1;  1   1   1]'
```

4.2. Realization of Step 2 and 3

The Step 2 and 3 can be realized using the following codes.

myTempTheta=mod(myTheta,pi/3);%Transform the phase myTheta in the interval $[0, \pi/3]$

myT1=sqrt(3)/2*myM*myPWMTs*sin(pi/3-myTempTheta);%First vector duration time
myT2=sqrt(3)/2*myM*myPWMTs*sin(myTempTheta); %Second vector's duration time
myT0=myPWMTs-myT1-myT2; % Zero vectors' total duration time
mySectorNo=fix(myTheta(i)/(pi/3))+1; %Sector No. where the command vector resides
if mySectorNo==1 | mySectorNo==3 | mySectorNo==5   % Sector 1,3 or 5
    myStartVector=myV(:,mySectorNo); % Start basic vector in Sector 1,3 or 5
    myEndVector=myV(:,mySectorNo+1); % End basic vector in Sector 1,3 or 5
else   % Sector 2,4 or 6
    myStartVector=myV(:,mod(mySectorNo+1,6));%Start basic vector in Sector 2,4 or 6
    myEndVector=myV(:,mySectorNo);% End basic vector in Sector 2,4 or 6
    myTempT=myT1; myT1=myT2;myT2=myTempT;% Change the duration time
end
myR0=0.5; % Partitioning ratio of the two zero basic vectors
SD=[myV(:,7),myStartVector,myEndVector,myV(:,8),myEndVector, myStartVector, ...
    myV(:,7)]; The matrix that should be concatenated to the vector sequence matrix S
myT00=myT0*myR0; myT07=myT0-myT00; % Each zero vector's duration time
STD=[myT00/2,myT1/2,myT2/2,myT07,myT2/2,myT1/2,myT00/2];
    %The matrix that should be concatenated to the time matrix ST
S=[S SD]; ST=[ST STD];   %Concatenate the matrixes

4.3. Realization of Step 4

   A variable FFTresult0 is set to store the previous results in Step 433 and Step 434. In order to combine Step 431 and 432, the initial value of FFTresult0 should be set large enough or small enough. The Step 4 can be realized using the following codes.
FFTResult0=100*ones(1,mySampleNumber/2); % Store the previous results
NumberFFTResult0= mySampleNumber/2; % Store the length of FFTResult0
NumberST=length(ST); % Get the length of the time matrix ST
STC=cumsum(ST); % Cumulate the sum of the elements of the time matrix ST
DS(:,1)=S(:,1); % Sample the first value
for myi0=1:100 % Maximum iterations is set to 100 here
    for myK0=1:NumberST
        myTemp1=fix((STC(myK0)-ST(myK0))/mySampDelataT);
        myTemp2=fix(STC(myK0)/mySampDelataT); %Compute the value range of r
        for myK1=(myTemp1+1):myTemp2
            DS(:,myK1+1)=S(:,myK0)* myHalfUdc; %Sample the value
        end
    end
    myUa=DS(1,:); myUb=DS(2,:); % Phase-A voltage , Phase-B voltage
    myFFTUa=fft(myUa-myUb)*2/mySampleNumber; % Discrete Fourier transform
    myFFTAmplitude=abs(myFFTUa); % Compute the amplitude
    FFTResult=myFFTAmplitude(2:NumberFFTResult0+1);% Get former values
    myError(myi0)=max(abs(FFTResult-FFTResult0))/   /FFTResult(1);%   Amplitude
error
    if myError(myi0)<2e-3 % The error limit is 2e-3 here
        break   % Terminate execution of FOR loop
    else   % The error is more than the set error limit
        FFTResult0=FFTResult; % Prepare for the next loop
        mySampleNumber=mySampleNumber*2; % The sampling number doubles.
   end
end

5. Examples and Results

For the commonly used symmetrical 7-segment SVPWM pattern of the two-level inverter, the partitioning ratio R_0 of the two zero basic space vectors is 0.5. That is to say, the two zero basic space vectors have the equal duration times, as the code "myR0=0.5" is used in Section 4.2. The DC bus voltage U_{DC} is 100V, the fundamental wave frequency is 60Hz, the switching frequency is 1800Hz and the error limit is 0.001. The harmonic spectrum of the line voltage between phase A and B and the computation error are shown in Figure 4 given that the modulation index M is 0.8.
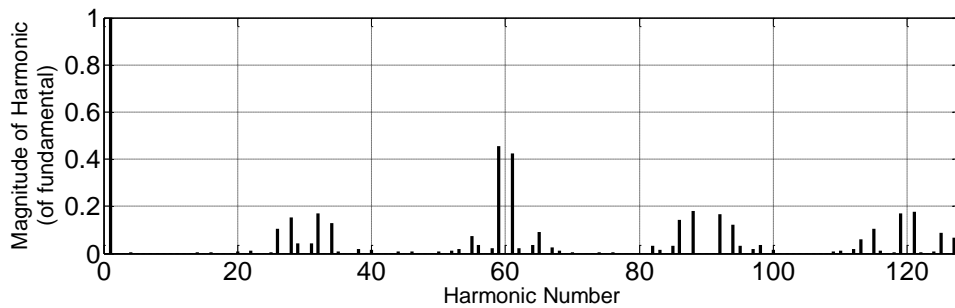
(a) Harmonic spectra of the line voltage between phase A and B plotted using the linear scale for both axes
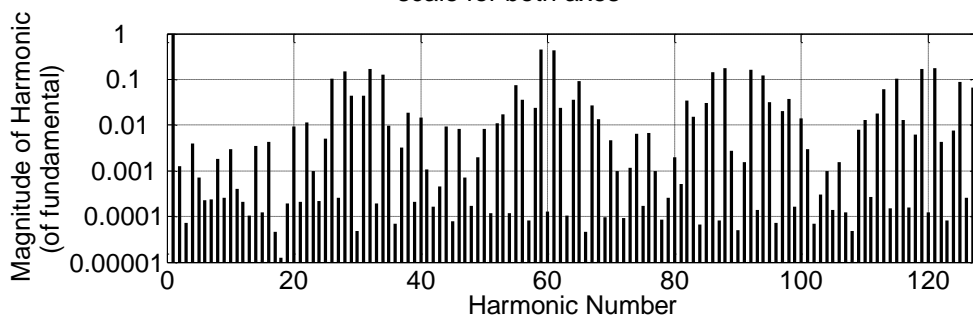
(b) Harmonic spectra of the line voltage between phase A and B plotted using a base 10 logarithmic scale for the Magnitude-axis and a linear scale for the Harmonic Number-axis
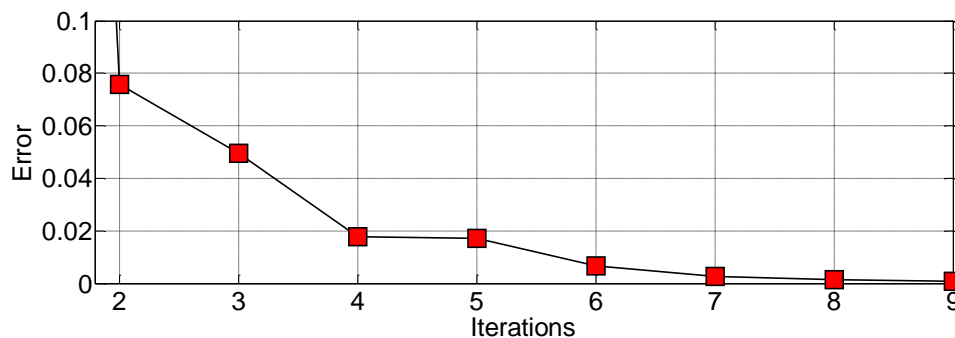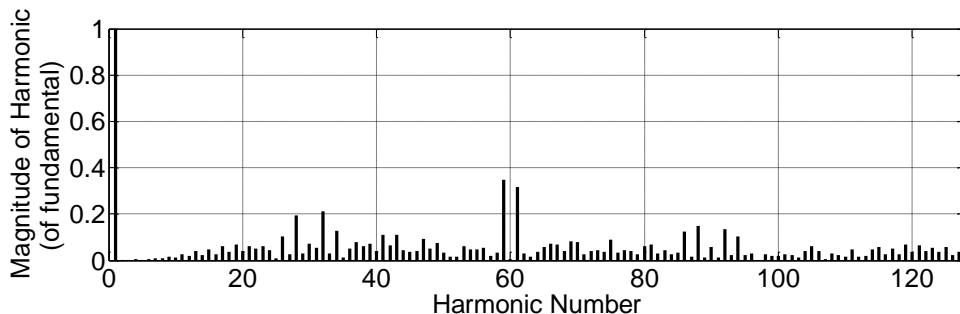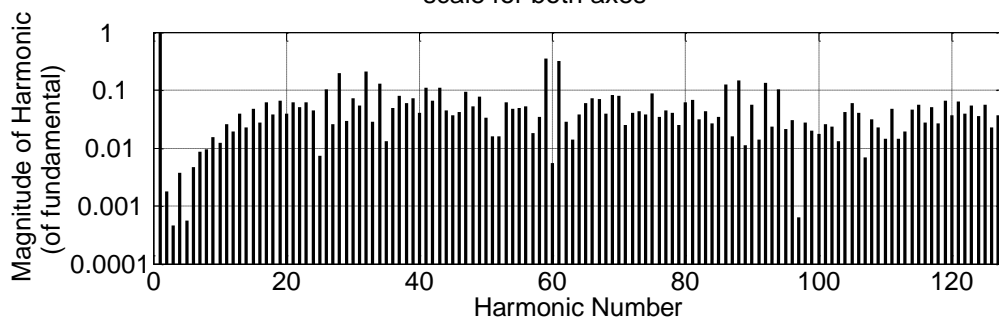

(c) Error as a function of iteration number

Figure 4. The Computation Results for the Symmetrical 7-Segment SVPWM Strategy

For the random zero-vector partitioning SVPWM strategy, the duration time ratio of the two zero basic vectors is a random variable. The code "myR0=0.5" in Section 4.2 should be replaced with a random number. For example, the function random that generates random arrays from a specified distribution can be used to generate the required random number. The command random('norm', A, B) returns a pseudorandom value

drawn from the uniform distribution on the open interval(A,B), and random('norm', A, B) can be replaced with the command (B-A)*rand. Given that the duration time ratio of the two zero basic vectors obeys a standard uniform distribution, the code "myR0=0.5" in Section 4.2 should be replaced with "myR0=rand", and the computation results are shown in Figure 5.

(a) Harmonic spectra of the line voltage between phase A and B plotted using the linear scale for both axes

(b) Harmonic spectra of the line voltage between phase A and B plotted using a base 10 logarithmic scale for the Magnitude-axis and a linear scale for the Harmonic Number-axis
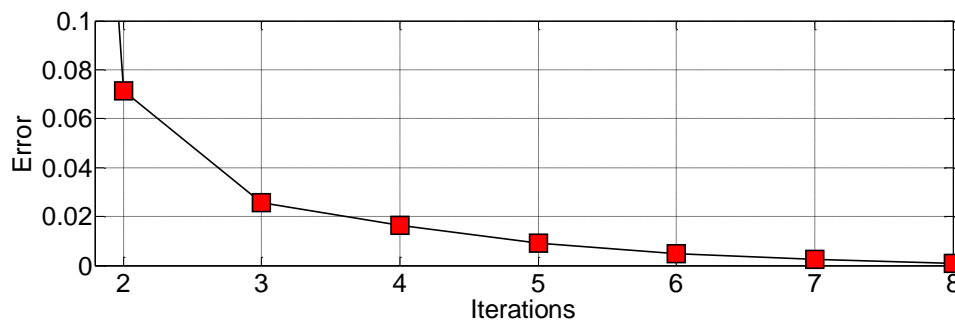
(c) Error as a function of iteration number

Figure 5. The Computation Results for the Random Zero-Vector Partitioning SVPWM Strategy

If the code "myR0=0.5" in Section 4.2 is replaced with "myR0=rand" and the code "STD=[myT00/2,myT1/2,myT2/2,myT07,myT2/2,myT1/2,myT00/2]" is replaced with "R1= rand; R2=rand; R3=rand; STD=[R1*myT00,R2*myT1,R3*myT2,myT07,(1-R3)*myT2,(1-R2)*myT1,(1-R1)*myT00]", the harmonic spectra of a hybrid SVPWM strategy of random zero-vector partitioning and pulse position can be got as shown in Figure 6.
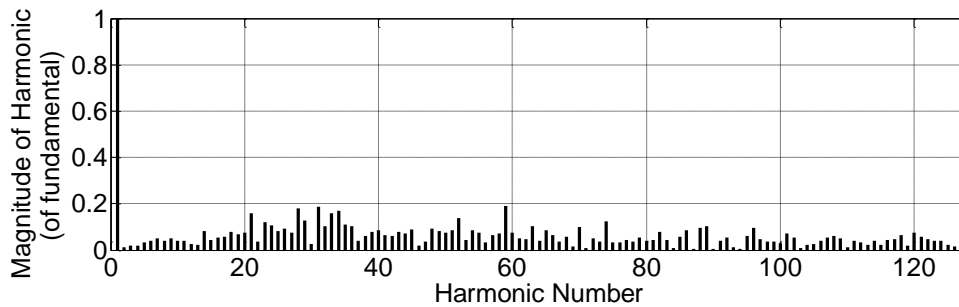
Figure 6. Harmonic Spectra of the Line Voltage between Phase A and B for A Hybrid SVPWM Strategy of Random Zero-Vector Partitioning and Pulse Position

The computing error decreases rapidly with the iteration increasing, which can be found from Figure 4(c) and Figure 5(c), and this shows that the proposed algorithm has excellent precision and efficiency. The remarkable harmonic spectrum difference between different SVPWM strategies can be found and compared easily. The random SVPWM strategy can significantly reduce the clustered harmonic magnitudes around the integer multiple switching frequencies. The peak magnitude around the 60th harmonic is more than 40% of that of the fundamental in the deterministic SVPWM strategy shown in Figure 4(a) and (b), while it is only less than 20% for the hybrid random strategy shown in Figure 6. The hybrid SVPWM strategy of random zero-vector partitioning and pulse position has better effect on reducing the clustered harmonic magnitudes than the random zero-vector partitioning one.

6. Conclusions

A computation algorithm to analyze the harmonic spectrum with adaptive precision for all kinds of SVPWM strategies is proposed. The key steps and codes are given in detail. The proposed algorithm and realization method in MATLAB have several features and advantages. Firstly, the algorithm does not depend on any specific SVPWM strategy, so it has sufficient convenience to analyze the harmonic spectrum of both the existing strategy and future new ones. In addition, the adaptive precision is realized through controlling the amplitude or magnitude error between the current result and the previous result. This is highly convenient and feasible because the true value of the spectrum is unavailable. If the computation error is less than the required limit, the computation terminates automatically. Finally, the realization method and key codes in MATLAB are presented and verified. The powerful functions and high precision features can be made full use of. The visualization function provides a powerful tool for comparing and analyzing the computation results at different levels. Because some harmonic magnitudes are very small or even nearly zero, the function semilogy is utilized to plot the magnitudes as logarithmic scales and the slight magnitude difference can be distinguished clearly. However, it should be noticed the FFT computation process is time consuming if the discrete time sequence includes too many elements, especially in case that the switching frequency is very high and the error limit is very small. If the current sampling voltage values and FFT results are made use of in the next iteration, the computation speed may be highly improved. This will be our future work.

Acknowledgments

References

[1] M. Xiaolin, J. A. Kumar and A. Rajapandian, "Hybrid interleaved space vector PWM for ripple reduction in modular converters", IEEE Transactions on Power Electronics, vol. 26, no. 7, **(2011)**, pp.1954-1967.

[2] D. G. Holmes and T. A. Lipo, "Pulse width modulation for power converters: principles and practice. IEEE Press, USA, **(2003)**.

[3] B. K. Bose, "Modern Power Electronics and AC Drives", Prentice Hall, UK **(2001).**

[4] G. Chen, "PWM Inverter Technology and Application", China Electric Power Press, China, **(2007)**.

[5] B. A. Rahiman, K. Saikrishna, A. H.Khalifa and D. Apparao, "Space-vector-based synchronized three-level discontinuous PWM for medium-voltage high-power VSI", IEEE Transactions on Industrial Electronics, vol. 61, no. 8, **(2014)**, pp. 3891-3901.

[6] R. P. Nagasekhara, A. J. and R. P. Linga, "Hybrid random PWM algorithm for direct torque controlled induction motor drive for reduced harmonic distortion", 2011 Annual IEEE India Conference: Engineering Sustainable Solutions (INDICON-2011), Hyderabad, India, **(2011)**.

[7] K. Shahriyar, M. Javad and A. Ali, "Application of random PWM technique for reducing the conducted electromagnetic emissions in active filters", IEEE Transactions on Industrial Electronics, vol. 54, no. 4, **(2007)**, pp. 2333-2343.

[8] S. H. Na, Y. G. Jung, Y. C. Lim and S. H. Yang, "Reduction of audible switching noise in induction motor drives using random position space vector PWM", IEE Proceedings Electric Power Applications, vol. 149, no. 3, **(2002)**, pp. 195-200.

[9] M. Zigliotto and A. M. Trzynadlowski, "Effective random space vector modulation for EMI reduction in low-cost PWM inverters", Proceedings of the 7th International Conference on Power Electronics and Variable Speed Drives, Stevenage, United Kingdom, **(1998)** September 21-23, pp. 163-167.

[10] N. Boudjerda, A. Boudouda, M. Melit, B. Nekhoul, E. K. Drissi and K. Kerroum, "Optimized dual randomized PWM technique for reducing conducted EMI in DC-AC converters", 10th International Symposium on Electromagnetic Compatibility(EMC Europe 2011), York, United kingdom, **(2011)**.

[11] D. Jiang and F.Wang, "Variable Switching Frequency PWM for Three-Phase Converters Based on Current Ripple Prediction", IEEE Transactions on Power Electronics, vol. 28, no. 11, **(2013)**, pp. 4951-4961.

[12] G. Chen, Z.Wu and Y. Zhu, "Harmonic Analysis of random pulse position space vector PWM", Journal of Tongji University, vol. 40, no. 7, **(2012)**, pp. 1111-1117.

[13] Z. Wu, G. Chen, Y. Zhu and G. Tian, "Harmonic analysis of random zero-vector distribution space vector pulse-width modulation", Journal of Tongji University, vol. 39, no. 9, **(2011)**, pp. 901-907.

[14] G. Chen, M. Zhang and J. Zhao, "Harmonic distortion factor of A hybrid space vector PWM based on random zero-vector distribution and random pulse position", Advances in Information Sciences and Service Sciences, vol. 4, no. 16, **(2012)**, pp. 242-250.

[15] S. Albatran, Y. Fu and A. Albanna, "Comprehensive mathematical description and harmonic analysis of hybrid two-dimensional-three-dimensional space vector modulation", IEEE Transactions on Industrial Electronics, vol. 61, no. 7, **(2014)**, pp. 3327-3336.

[16] G. Chen and J. Kang, "A Spectrum Analysis Method to Space Vector Pulse Width Modulation", Advanced Science and Technology Letters, vol. 134, **(2016)**, pp. 164-167.

[17] J. Holtz, M. Holtgen and J. O. Krah, "A Space Vector Modulator for the High-Switching Frequency Control of Three-Level SiC Inverters", IEEE Transactions on Power Electronics, vol. 29, no. 5, **(2014)**, pp. 2618-2626.

[18] N. Celanovic and D. Boroyevich, "A Comprehensive Study of Neutral-Point Voltage Balancing Problem in Three-Level Neutral-Point-Clamped Voltage Source PWM Inverters", IEEE Transactions on Power Electronics, Vol. 15, No. 2, **(2000)**, pp. 242-249.

[19] L. H. Dai, X. B. Chen, Z. J. Yu and Y. J. Fu, "Three-level inverter and its simulation", Journal of University of Sciences and Technology Liaoning, vol. 34, no. 1, **(2011)**, pp. 360-367.

Authors
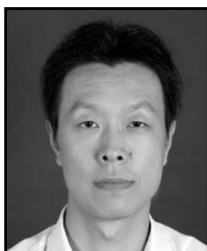
Guoqiang Chen is currently an associate professor in the School of Mechanical and Power Engineering, Henan Polytechnic University, China. His research interests include robot technology, electric vehicle control, motor control and pulse width modulation technology.